

Observation of OAM sidebands due to optical reflection

W. Löffler,^{1,*} Andrea Aiello,^{2,3} and J. P. Woerdman¹

¹*Huygens Laboratory, Leiden University, P.O. Box 9504, 2300 RA Leiden, The Netherlands*

²*Max Planck Institute for the Science of Light, Günther-Scharowsky-Straße 1/Bldg. 24, 91058 Erlangen, Germany*

³*Institute for Optics, Information and Photonics, Universität Erlangen-Nürnberg, Staudtstr. 7/B2, 91058 Erlangen, Germany*

We investigate how the orbital angular momentum (OAM) of a paraxial light beam is affected upon reflection at a planar interface. Theoretically, the unavoidable angular spread of the (paraxial) beam leads to OAM sidebands which are found to be already significant for modest beam spread (0.05). In analogy to the polarization Fresnel coefficients we develop a theory based upon spatial Fresnel coefficients; this allows straightforward prediction of the strength of the sidebands. We confirm this by experiment.

PACS numbers:

A light beam, either classical or quantum, possesses spatially transverse degrees of freedom. A very popular example is the Orbital Angular Momentum (OAM) of light [1, 2]; this has important applications in quantum communication [3–5]. The key advantage of OAM for quantum communication is its high dimensionality [6]; this allows a single photon to carry much more [7, 8] than the two bits of information (qubit) enabled by the polarization degree of freedom. In this Letter we investigate, theoretically and experimentally, the effect of optical reflection at a planar interface on the OAM state of a beam. This is a relevant issue since reflection is the simplest possible optical operation, and is often unavoidable in experiments and applications. An analogous issue is well known for the case of light’s polarization; this is generally strongly affected by Fresnel reflection (apart from special cases [32]). What happens in the OAM case? Everyday experience tells us that image distortion does not occur if we use a planar mirror; this suggests that the spatial state of the input beam (and thus also the OAM spectrum) should be well preserved upon reflection.

As we will see, the OAM state is indeed conserved if we use an ideal mirror, which we define as a (planar) mirror with infinite dielectric contrast. However, a practical mirror has a finite dielectric contrast; think for instance of a single dielectric interface, or a multi-layer dielectric mirror, or a metal mirror. In this case wave optics leads to diffractive corrections upon Snell’s Reflection Law such as the Goos-Hänchen [9] (GH) and Imbert-Fedorov [10, 11] (IF) shifts: the reflected beam is shifted relative to the geometrical-optics reflected ray [12–17]. A natural theoretical description is furnished by spatial Fresnel coefficients that act upon the transverse modes of the incident light beam, analogous to the conventional polarization Fresnel coefficients that act upon the polarization modes. We find that the reflection-induced modification of the OAM state depends on the angular spread of the beam; this leads to OAM sidebands, even in the

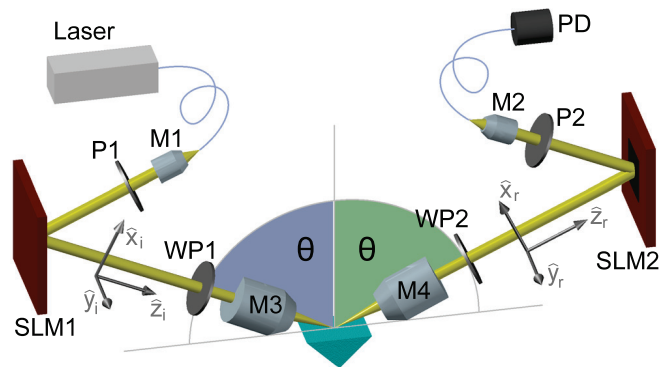


Figure 1: Experimental setup: Light from a single mode fiber pigtailed laser is collimated (M1), polarized (P1), and then modulated using a phase-only spatial light modulator (SLM1) to prepare a certain mode. This light is then reflected at the interface, and the reflected light is analyzed using a combination of SLM2 and a single mode fiber connected to a photodiode (PD). Microscopy objectives M3 & M4 (10x, 0.25 NA) can be introduced to change the beam focussing (θ), $\lambda/2$ waveplates WP1&2 modulate the polarization.

paraxial approximation. This is confirmed by our experimental results.

Our work connects with several papers that report on OAM spectral broadening due to misalignment of the reference frame with respect to the OAM beam [8, 18, 19]. In an experiment this type of broadening can obviously be removed by proper re-adjustment of the set-up to compensate the original misalignment. However, in our case we deal with intrinsic displacements (due to GH and IF shifts); this case is essentially different since, as we will see, intrinsic displacement depends on the spatial (OAM) mode and can thus not be cancelled simply by optical adjustment if we deal with a superposition of spatial modes as input state. We aim here to quantify the corresponding OAM spectral broadening. Our work also connects with that of Okuda and Sasada [20, 21] who study gi-

ant (nonperturbative) deformation of a OAM mode due to total internal reflection (TIR) for incidence very close to the critical angle, where a singularity occurs. In this regime beam shifts (GH and IF) and thus the OAM mode spectrum are ill-defined concepts [21]; we do not consider this singular TIR case in the present Letter.

Theoretically, we describe the reflection process in terms of a scattering operator $\hat{S} = \sum_{\lambda} \hat{P}_{\lambda} \otimes \hat{M}_{\lambda}$, where \hat{P}_{λ} acts on the polarization state $|\lambda\rangle$ ($\lambda = 1$ and $\lambda = 2$ correspond to p (in plane) and s (out of plane) polarization, respectively), and \hat{M}_{λ} on the spatial state $|\psi\rangle$. Here we have adopted a quantum notation for the sake of clarity. We restrict ourselves to a paraxial light field, in this case polarization and spatial degree of freedom factorize: $|in\rangle = |\lambda\rangle|\psi\rangle$. Upon reflection, \hat{S} mixes the polarization and spatial part; thus after scattering, it is not possible to write the state as before in a product of polarization times spatial state [17, 22]; further this enables the link between beam shifts and weak measurements [13, 23].

In more detail, we discuss the incoming field $\mathbf{E}_i(x_i, y_i, z_i, t) = \text{Re}[\mathbf{A}_i(x_i, y_i, z_i) \exp(-i\omega t)]$ in terms of its *analytic signal* [24–26] $\mathbf{A}_i(x_i, y_i, z_i) = \sum_{\lambda} a_{\lambda} \hat{\mathbf{e}}'_{\lambda} \psi(x_i, y_i, z_i)$ where ψ describes the spatial shape of the beam (which we keep arbitrary at this point), $\hat{\mathbf{e}}'_1 = \hat{\mathbf{x}}_i$ and $\hat{\mathbf{e}}'_2 = \hat{\mathbf{y}}_i$, are the incoming-beam unit vectors, and $a_{1,2}$ are the polarization coefficients. All coordinates are expressed in units of k , and hence dimensionless. The reflected field can be written as

$$\mathbf{A}(x, y, z) = \sum_{\lambda} a_{\lambda} r_{\lambda}(\theta) \psi(-x + X_{\lambda}, y - Y_{\lambda}, z) \hat{\mathbf{e}}_{\lambda} \quad (1)$$

where $\hat{\mathbf{e}}_1 = \hat{\mathbf{x}}_r$ and $\hat{\mathbf{e}}_2 = \hat{\mathbf{y}}_r$ are the unit vectors in the reflected-beam coordinate system (Fig. 1). The reflected field \mathbf{A} depends on the Fresnel reflection coefficients r_{λ} and the four complex beam shifts X_{λ} and Y_{λ} , whose real (imaginary) part corresponds to spatial (angular) longitudinal Goos-Hänchen [9] and transverse Imbert-Fedorov [11, 12] shifts, respectively [25]: $X_{\lambda} = -i \partial_{\theta} [\ln r_{\lambda}(\theta)]$ and $Y_1 = -i \frac{a_2}{a_1} \left(1 + \frac{r_2}{r_1}\right) \cot \theta$, $Y_2 = i \frac{a_1}{a_2} \left(1 + \frac{r_1}{r_2}\right) \cot \theta$. By analyzing X_{λ} and Y_{λ} it can easily be seen that only an infinite refractive index contrast makes them disappear, so only at reflection from such a perfect mirror, the reflected mode $\mathbf{A}(x, y, z)$ is not perturbed. Since the combined shift $\mathbf{R}_{\lambda} = (X_{\lambda}, Y_{\lambda})$ is supposedly small, we can Taylor-expand the shifted function ψ to find deviations from geometrical optics reflection. We obtain for the spatial part with $\mathbf{R} = (x, y)$:

$$\begin{aligned} \langle x, y, z | \hat{M}_{\lambda} | \psi \rangle &= \psi(-x + X_{\lambda}, y - Y_{\lambda}, z) \\ &\simeq \psi(-x, y, z) + \mathbf{R}_{\lambda} \cdot \frac{\partial}{\partial \mathbf{R}} \psi(-x, y, z) \end{aligned} \quad (2)$$

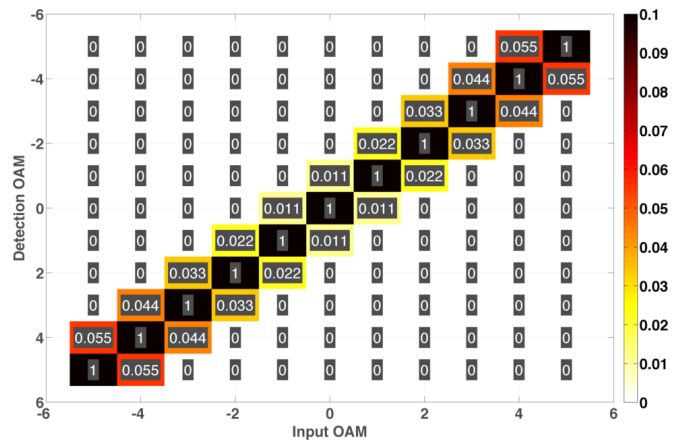


Figure 2: Calculated SFC intensity $C_{\ell, \ell'}^p = |c_{\ell, \ell'}^p|^2$ for the case of p -polarized OAM modes externally reflected at a dielectric interface ($n = 1.52$, $\theta = 70^\circ$, $\theta_0 = 0.05$). Input (ℓ) and output (ℓ') OAM is shown on the horizontal and vertical axis, respectively (radial mode number $p = 0$).

Now, we specialize to a specific mode basis, and expand the spatial part of the input field in terms of the Laguerre-Gauss modes ϕ_{ℓ}^p as $|\psi\rangle = \sum_{\ell, p} |\phi_{\ell}^p\rangle \langle \phi_{\ell}^p | \psi \rangle$. Our goal is to predict the reflected state, from which we can derive the spatial mode scattering matrix \hat{M}_{λ} , which has as elements the spatial Fresnel coefficients (SFC)

$$c_{\ell, p, \ell', p'}^{\lambda} \equiv \langle \phi_{\ell'}^{p'} | \hat{M}_{\lambda} | \phi_{\ell}^p \rangle \quad (3)$$

To obtain these coefficients, we use two properties of LG modes: (i) $\phi_{\ell}^p(-x, y, z) = (-1)^{\ell} \phi_{-\ell}^p(x, y, z)$ and (ii) the known spatial derivatives of LG modes, $\frac{\partial \phi_{\ell}^p}{\partial x}$ and $\frac{\partial \phi_{\ell}^p}{\partial y}$, up to first order in θ_0 ($= \lambda/\pi\omega_0$), the mode half-opening angle. We find the following non-zero coefficients $c_{\ell, p, \ell', p'}^{\lambda}$:

$p' \backslash \ell' (\ell' \geq 0)$	$-\ell \mp 1$	$-\ell$	$-\ell \pm 1$
$p - 1$	$\pm Z_{\lambda}^{\pm} \sqrt{p}$	0	0
p	$\pm Z_{\lambda}^{\pm} \sqrt{ \ell + p + 1}$	$(-1)^{\ell}$	$\mp Z_{\lambda}^{\mp} \sqrt{ \ell + p}$
$p + 1$	0	0	$\mp Z_{\lambda}^{\mp} \sqrt{p + 1}$

$p' \backslash \ell' (\ell' = 0)$	-1	0	+1
$p - 1$	$Z_{\lambda}^{+} \sqrt{p}$	0	0
p	$Z_{\lambda}^{+} \sqrt{p + 1}$	$(-1)^{\ell}$	$-Z_{\lambda}^{-} \sqrt{p}$
$p + 1$	0	0	$-Z_{\lambda}^{-} \sqrt{p + 1}$

Here, we can elegantly combine all occurring shifts, i.e., the longitudinal and transverse, in each case the spatial and angular variant, in a single complex number

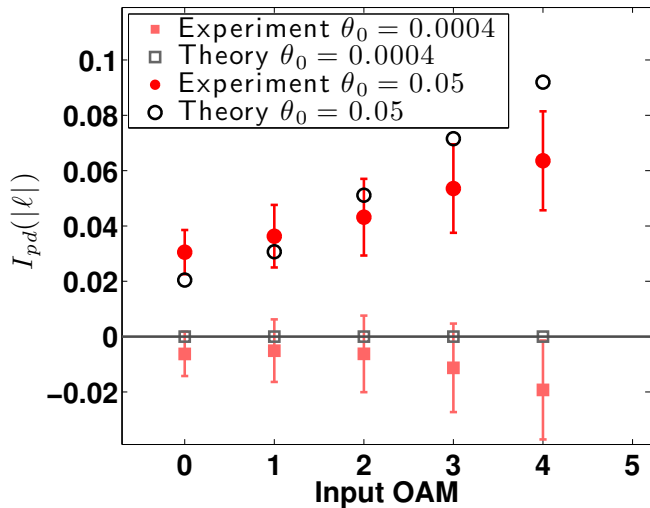


Figure 3: Experimental and theoretical polarization-differential SFC sideband intensity $I_{pd}(\ell)$ as a function of input OAM (ℓ) for $p = 0$, for the case of external reflection by an air-glass interface, at an angle of incidence $\theta = 70^\circ$. Error bars are estimated from multiple measurement runs to take mechanical drifts and misalignment into account.

$Z_\lambda^\pm = \frac{\theta_0}{2^{3/2}} (-1)^\ell (X_\lambda \pm i Y_\lambda)$. This is specific to Laguerre-Gauss modes. Fig. 2 shows exemplary the SFC intensities $C_{\ell,\ell'}^p = |c_{\ell,\ell'}^p|^2$ for reflection of p-polarized purely azimuthal ($p = 0$) LG modes with $\theta_0 = 0.05$ at an angle of incidence of $\theta = 70^\circ$ under external reflection at an air-BK7 interface. We find that reflection described by the SFCs induces a transformation of a pure $\{\ell\}$ mode into a superposition of $\{-\ell - 1, -\ell, -\ell + 1\}$ modes, where the minus sign stems simply from OAM reversal upon reflection. The coupling strength to the OAM sideband modes $\{-\ell - 1, -\ell + 1\}$ is proportional to θ_0^2 and depends linearly on ℓ . In our case of pure azimuthal modes, the coupling strength is simply proportional to $(\theta_0 \sqrt{|\ell|})^2$; here we recognize the effective mode opening angle of which is proportional to $\theta_0 \sqrt{|\ell|}$. We also see that the mode coupling is governed by intrinsic displacement induced by beam shifts X_λ and Y_λ . In the particular case of external reflection at a dielectric, only angular beam shifts occur [12, 14]; this can be seen by analyzing X_λ and Y_λ : for linear s or p polarization, Y_λ vanishes, and X_λ is purely imaginary, this corresponds to an angular shift within the plane of incidence.

The discussion above was for the case of a single OAM input state; however it is straightforward to extend this to an OAM superposition input state. The mode coupling by reflection is a coherent scattering process so that a superposition can be handled by decomposition into its constituent OAM modes.

As a demonstration experiment, we investigate the case displayed in Fig. 2, i.e. external reflection at an air - glass

interface. As shown in Fig. 1, light from a fiber pig-tailed 635 nm laser is collimated using a 20x microscopy objective (beam waist $\omega_0 = 530 \mu\text{m}$, this corresponds to $\theta_0 = 0.0004$). The light is sent to a spatial light modulator (SLM1) ($10 \mu\text{m}$ pixel size, 3 mrad blaze angle), which imprints the desired azimuthal phase to produce the input OAM spectrum (ℓ ; $p = 0$). The beam is then focused, externally reflected at the hypotenuse plane of a standard BK7 ($n = 1.52$) glass prism, and then recollimated to a beam waist of $\omega_0 = 530 \mu\text{m}$. For this telescope configuration we use underfilled 10x microscopy objectives (to minimize aberrations) M3 and M4 (0.25 NA) to obtain $\theta_0 = 0.05$ inside the telescope, which is well within the paraxial approximation. The reflected beam $[out]$ is sent to SLM2 (phase profile ℓ') which is followed by microscopy objective M4 and a single-mode fiber; thus we project on a pure OAM mode (ℓ') [33]. The fiber is connected to a photodiode (PD); its photocurrent is proportional to $C_{\ell,\ell'}$. By scanning the OAM of the input (ℓ) and output (ℓ') modes, we map the matrix containing the spatial Fresnel coefficients. From these data we deduce the relative intensity in the OAM sidebands compared to the total reflected intensity

$$I_{rel}^\lambda(\ell) = \frac{C_{\ell,-\ell-1}^\lambda + C_{\ell,-\ell+1}^\lambda}{\sum_{\ell'} C_{\ell,\ell'}^\lambda} \quad (5)$$

In order to improve the signal-to-noise ratio we use polarization modulation (s versus p) with a half-wave plates (WP1 and WP2) before and after reflection from the interface; this enables polarization-differential measurement. The experiment thus yields the polarization-differential $I_{pd}(\ell) = I_{rel}^p(\ell) - I_{rel}^s(\ell)$, which is plotted in Fig. 3 versus the input ℓ , at a fixed angle of incidence ($\theta_0 = 70^\circ$). The data for $\theta_0 = 0.0004$ have been obtained without the telescope. In this case Eq. 4 predicts polarization-differential sidebands $< 10^{-5}$ in the experimentally addressed ℓ range, which is much smaller than (but consistent with) the experimental accuracy. For $\theta_0 = 0.05$ the mode coupling is increased, in reasonable agreement with theory [34]. From experiments, as well as from numerical simulation, we observe that mode coupling to $-\ell \pm 2$ modes is at least an order of magnitude smaller than the coupling to $-\ell \pm 1$ [35].

In Fig. 4a we present calculations of the SFC sidebands for $\ell = 4$, for the full range of angles of incidence, for s and p polarization separately, as well as for the polarization-differential case. For p polarization a Brewster resonance occurs due to the vanishing of the reflection [27] making its contribution to the sidebands in most cases much larger than that of s -polarization; i.e. the polarization-differential $I_{pd}(\ell)$ is a sensible measure. For $\theta_0 = 0.0004$ this admixture is (far) below 0.01, except in a very narrow (0.5°) angular window centered at the Brewster angle.

It is interesting to compare our results for an air-glass interface with other cases, such as an air-metal interface. Our theory is fully adequate for this since the material properties enter only via the refractive index (or dielectric constant) which is complex-valued for a metal. Fig. 4b gives the SFC sidebands $I_{pd}(\ell = 4)$ for a silver interface ($n_{Ag} = 0.14 + 4i$ at $\lambda = 635$ nm). In the collimated case, the sideband intensity is now much smaller ($< 10^{-5}$ at all angles of incidence) than for an air-glass interface, basically since a metal is a much better reflector. Also, the Brewster resonance is absent in this case. We expect similar results for a dielectric Bragg mirror. It will be interesting to check these predictions experimentally.

In conclusion, we have introduced the concept of spatial Fresnel coefficients (SFC) to describe transverse-mode dependent reflection of a light beam. In the OAM basis we find that an OAM mode $\{\ell\}$ acquires sidebands. The sidebands are due to first-order diffractive corrections to geometric optics (GH and IF effects); these lead to mode-dependent displacement and thus to coupling to “neighboring” OAM modes. We find that these effects scale with the angular spread of the beam. Only for well collimated beams they are small, which bodes well for the use of folding mirrors in optical set-ups in the laboratory and for mirror-assisted free-space OAM communication; contrarily, the polarization degree of freedom can be severely complicated by intervening mirrors.

The OAM sidebands are enhanced for already moderately focussed beams. We have used this case to validate our theory, by measuring the sidebands occurring during external reflection by an air-glass interface, still staying within the paraxial approximation. Practically, this case could be encountered in the laboratory when using a beam splitter to pick off a weak copy of a focused OAM light beam. The sidebands disappear only in the limit of an ideal mirror with an infinite refractive index step.

An intriguing question is, can we undo the SFC-induced mode coupling? The reflective scattering process described by the matrix $c_{\ell,\ell'}^\lambda$ is reversible, so that in principle superposition input states can be recovered with unity fidelity. But how can this be achieved experimentally? An ordinary mirror cannot do this since it simply adds to the diffractive beam shifts (GH and IF). We thus need an optical device that cancels intrinsic beam shifts; possibly a negative-index metamaterial [28–30] or photonic crystal [31] could achieve this task.

We acknowledge fruitful discussions with M. J. A. de Dood, J. B. Götte, and G. Nienhuis, and financial support by NWO and the EU STREP program 255914 (PHORBITECH).

BIBLIOGRAPHY

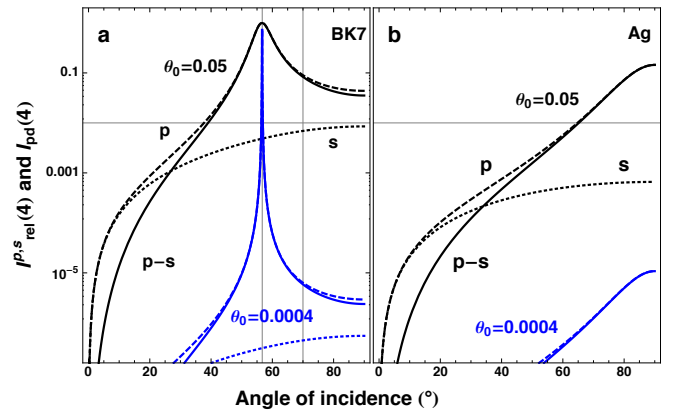


Figure 4: The relative $I_{rel}^{p,s}(\ell = 4)$ and polarization-differential $I_{pd}(\ell = 4)$ intensity of the OAM sidebands (theory, logarithmic plots) for external reflection. (a) shows the case for an air-BK7 interface ($n = 1.52$), and (b) for a silver mirror; gray curves for $\theta_0 = 0.0004$ (“collimated”) and black curves for $\theta_0 = 0.05$. We see that in case of the glass interface, the experimentally accessible polarization-differential sideband intensity (continuous curve) is dominated by p polarization (dashed curve), since s polarization (dotted line) does not experience the Brewster resonance. The vertical lines indicate the Brewster angle and the angle for which we show measurements in Fig. 3.

* Electronic address: loeffler@physics.leidenuniv.nl

- [1] L. Allen, M. W. Beijersbergen, R. J. C. Spreeuw, and J. P. Woerdman, Phys. Rev. A **45**, 8185 (1992).
- [2] L. Allen, M. Padgett, and M. Babiker (Elsevier, 1999) pp. 291 – 372.
- [3] A. Mair, A. Vaziri, G. Weihs, and A. Zeilinger, Nature **412**, 313 (2001).
- [4] G. Molina-Terriza, J. P. Torres, and L. Torner, Nat. Phys. **3**, 305 (2007).
- [5] A. C. Dada, J. Leach, G. S. Buller, M. J. Padgett, and E. Andersson, Nat. Phys. **7**, 677 (2011).
- [6] B.-J. Pors, F. Miatto, G. W. ’t Hooft, E. R. Eliel, and J. P. Woerdman, J. Opt. **13**, 064008 (2011).
- [7] H. Bechmann-Pasquinucci and W. Tittel, Phys. Rev. A **61**, 062308 (2000).
- [8] G. Gibson, J. Courtial, M. Padgett, M. Vasnetsov, V. Pas’ko, S. Barnett, and S. Franke-Arnold, Opt. Express **12**, 5448 (2004).
- [9] F. Goos and H. Hänchen, Ann. Phys. **436**, 333 (1947).
- [10] F. I. Fedorov, Dokl. Akad. Nauk SSSR **105**, 465 (1955).
- [11] C. Imbert, Phys. Rev. D **5**, 787 (1972).
- [12] K. Y. Bliokh and Y. P. Bliokh, Phys. Rev. Lett. **96**, 073903 (2006).
- [13] O. Hosten and P. Kwiat, Science **319**, 787 (2008).
- [14] A. Aiello and J. P. Woerdman, Opt. Lett. **33**, 1437 (2008).
- [15] H. G. L. Schwefel, W. Köhler, Z. H. Lu, J. Fan, and L. J. Wang, Opt. Lett. **33**, 794 (2008).
- [16] H. Gilles, S. Girard, and J. Hamel, Opt. Lett. **27**, 1421 (2002).
- [17] K. Y. Bliokh and Y. P. Bliokh, Phys. Rev. E **75**, 066609

- (2007).
- [18] M. V. Vasnetsov, V. A. Pas'ko, and M. S. Soskin, *New J. Phys.* **7**, 46 (2005).
- [19] R. Zambrini and S. M. Barnett, *Phys. Rev. Lett.* **96**, 113901 (2006).
- [20] H. Okuda and H. Sasada, *Opt. Express* **14**, 8393 (2006).
- [21] H. Okuda and H. Sasada, *J. Opt. Soc. Am. A* **25**, 881 (2008).
- [22] A. Aiello and J. P. Woerdman, *Phys. Rev. A* **70**, 023808 (2004).
- [23] M. R. Dennis and J. B. Götte, pre-print (2012), arXiv:1204.0327 .
- [24] K. Y. Bliokh, I. V. Shadrivov, and Y. S. Kivshar, *Opt. Lett.* **34**, 389 (2009).
- [25] M. Merano, N. Hermosa, J. P. Woerdman, and A. Aiello, *Phys. Rev. A* **82**, 023817 (2010).
- [26] A. Aiello, *New J. Phys.* **14**, 013058 (2012).
- [27] M. Merano, A. Aiello, M. P. van Exter, and J. P. Woerdman, *Nat. Photon.* **3**, 337 (2009).
- [28] P. R. Berman, *Phys. Rev. E* **66**, 067603 (2002).
- [29] A. Lakhtakia, *Electromagnetics* **23**, 71 (2003).
- [30] G. Dolling, M. W. Klein, M. Wegener, A. Schädle, B. Kettner, S. Burger, and S. Linden, *Optics Express* **15**, 14219 (2007).
- [31] J. He, J. Yi, and S. He, *Opt. Express* **14**, 3024 (2006).
- [32] Only the eigenstates, s or p polarization, remain pure upon reflection, albeit attenuated
- [33] The reflected-beam axis is adjusted to be the axis of the reflected s-polarized fundamental Gaussian beam.
- [34] Experimental errors are ascribed to drift and residual misalignment; apart from proper adjustment of the setup and the holograms we had to align very precisely the orientation and position of the microscopy objectives, and stability is of extreme importance.
- [35] The Brewster angle is at $\theta_B = 56.7^\circ$. In Fig.3 we show results for an angle of incidence of $\theta = 70^\circ$, this is $5 \cdot \theta_0$ separated from the Brewster resonance [27] at $\theta_B = 56.7^\circ$, thus we operate truly in the perturbative regime.